



ELSEVIER

International Journal of Mass Spectrometry 206 (2001) 275–286



Recent progress in matrix-assisted laser desorption ionization postsources decay

Jochen Franzen, Rüdiger Frey, Armin Holle, Karl-Otto Kräuter

Ulrike Schweiger-Hufnagel, Detlev Suckau, Bruker Daltonik GmbH Bremen, and Aurelio La Rotta, Universität Bonn, Bonn, Germany

Received 25 May 2000, accepted 11 December 2000

Abstract

In matrix-assisted laser desorption and ionization mass spectrometry, using a time-of-flight analyzer, decomposition of analytes by postsources decay can be examined by making use of an electrostatic ion reflector, thus recording tandem mass spectra. In recent years reasonable progress has been made using different instrument configurations and different types of reflectors. Also, the resolution of the first mass spectrum, i.e. the resolution of the precursor ion selector and the speed and possibility of automation of the acquisition and interpretation of the data has been improved. This article reviews the work of different groups working in this field and discusses the advantages of various arrangements. (Int J Mass Spectrom 206 (2001) 275–286) © 2001 Elsevier Science B.V.

Keywords: MALDI; PSD; CID; TOF; Tandem mass spectra

1. Introduction and short outline of matrix-assisted laser desorption and ionization postsources decay

An excellent overview on mass spectrometry and its applications is presented in the 1998 review article “Mass Spectrometry” by A. L. Burlingame, R. K. Boyd, and S. J. Gaskell [1]. A 1999 report on “New Time-of-Flight Mass Spectrometry” by Robert J. Cotter describes improved performance of modern TOF spectrometers [2]. The present progress report focuses on some recent improvements in postsources decay (PSD) measurements with matrix-assisted laser desorption and ionization (MALDI) time-of-flight (TOF) instruments achieved during the last two years.

The acquisition of fragment ion spectra of selected parent ions generated by MALDI roots back to Kaufmann and his group at the university of Düsseldorf [3,4]. Kaufmann used the Mamyrin ion reflector of TOF mass spectrometers to analyze fragment ions generated by PSD of parent ions along the field-free flight path toward the reflector. The metastable decay is caused by excess ion energy obtained during the complex MALDI process.

Typically, PSD spectra are acquired as a series of spectra taken at different reflector potentials for the following reason: After leaving the ion source all ions have the same kinetic energy, besides an internal energy obtained from various mechanisms like laser irradiation, gas phase collisions, etc. During their flight in the field-free region there is a long time available (microsecond time scale) for fragmentation due to this high internal energy. The produced frag-

* Corresponding author. E-mail: Armin.Holle@bdal.de

ment ions basically keep the same velocity, but since the kinetic energy of the fragment ions is proportional to their respective mass, it is only a fraction of the precursor kinetic energy. Due to this mass-dependent kinetic energy, PSD ions are reflected at different potentials, i.e. different locations in the reflector and their flight time vary although their speed remains unchanged. Therefore, in PSD the reflector acts as a kinetic energy analyzing device in contrast to normal mass spectrometry measurements where all ions have the same kinetic energy but their velocity is a function of mass (m/z).

Because the two-stage Mamyrin reflector typically used for PSD can reflect only a restricted mass range of about 20%–40% of the precursor mass with sufficient resolution, fragment ions with lower masses have to be “energy analyzed” at lower reflector potentials. This means, the full fragment ion spectrum has to be acquired in several spectrum segments each taken at an approximately 20%–40% lower reflector potential than the previous one. Depending on the lowest mass of interest, 5–20 segment spectra may have to be acquired and concatenated to represent a full daughter or fragment ion spectrum.

In order to acquire a fragment ion spectrum of a single precursor or parent ion mass from a complex mixture such as an enzymatic protein digest, exclusively this mass has to be selected. Since the precursor ions of different masses have a different velocity, they pass the selector at different times. Therefore, a time-of-flight selector is very suitable, which allows the ion passage only during a very restricted time window. This “precursor ion selector” is a shutter gate between ion source and reflector which allows the transmission of the selected parent ions together with respective daughter ions formed prior to the selector passage and travel with the same speed (details given in Fig. 1 and in the following).

Time-of-flight mass spectrometry with MALDI ionization experienced a breakthrough by the enhancement of mass resolution and precision introduced by a method called “space–velocity correlation focusing” (SVCF) by their inventors [5], based on the 40 year old procedure of “time-lag focusing” by Wiley and McLaren [6], transferred from electron

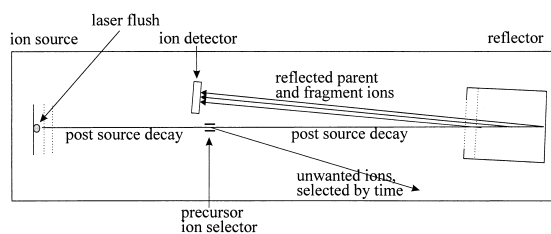


Fig. 1. Principle of fragment ion spectrum acquisition by postsource decay of parent ions in the first field-free flight path (PSD with MALDI-TOF).

beam ionization with pulsed ion extraction to modern MALDI, and intermediate improvements [7]. This method has become known under different names: “delayed extraction” (DE) or “pulsed ion extraction.” The acceleration field for the MALDI-generated ions is only switched on several hundred nanoseconds after the laser pulse. The effect of SVCF is not purely an effect of better focusing, we rather see the main improvement of mass accuracy in the fact, that during the time delay the protonation for high mass ions can be completed prior to acceleration; only then the space and velocity distributions of the ions are strongly correlated. The basic time focusing effect of SVCF is simple: ions of higher original energy see a lower potential at the inset of the acceleration and thus gain lesser energy in the acceleration field, so that the originally slower ions can catch up with the originally faster ions; a time focus for ions of the same mass is formed.

The enhanced mass precision revolutionized TOF mass spectrometry and opened its application to proteomics and others, where TOF mass spectrometry has since become a major tool in the identification of proteins by their enzymatic mass fingerprint and PSD patterns of selected proteolytic peptides in protein sequence library searches.

If fingerprint comparisons do not yield unique identification results, or give no identification at all, fragment ion spectra reveal the sequence of a selected proteolytic peptide. The fragment ion spectra allow for unambiguous identification and can even be used for de novo sequencing.

Current developments in tandem mass spectrometry TOF methods concentrate in the following

areas: improvement of precursor ion selection, automation of segmented PSD spectrum acquisition and calibration, instrumental developments to get full and nonsegmented PSD [or collisionally induced decomposition (CID)] daughter ion spectra from MALDI ions, derivatizing of peptides to get simpler spectra from PSD, and improvement of sample preparation techniques, supports, and matrices for MALDI and MALDI PSD.

2. Improved precursor ion selection

In case of analyses from individual components in mixtures, these must be exclusively selected before they can be PSD analyzed. All other precursor masses have therefore to be eliminated, usually by a time gating device within the first field-free path of the spectrometer, called a “precursor ion selector.” This device deflects all ions by a permanent electrostatic field orthogonal to the ion axis. The deflecting field is switched off only for a short period of time, during which the selected parent ions pass the selector as well as their respective fragment ions, which have the same velocity.

The deflection gates are usually operated with so-called push–pull voltage devices. These voltage generators can switch off the deflection voltage within a few nanoseconds, keep the zero voltage for an adjustable time of nanoseconds to microseconds, and switch the voltage back in nanoseconds. Mass resolution of these gating devices is around $m/\Delta m=100$ full width at half maximum (FWHM), sufficient to select a peptide and discriminate the oxidated (+16 u) species up to 1600 u. To achieve even this moderate resolution, the time focus of the space–velocity correlation focusing of the ion source has to be adjusted to match the position of the precursor ion selector. Because this resolution of the precursor ion selector represents a major limit for PSD of ions in complex mixtures, great efforts went into the development of higher resolution ion selectors (see Fig. 2).

A fundamentally new idea for improvement came from Barofsky and co-workers [8]: they switched the voltage of the deflection device to the adverse polarity

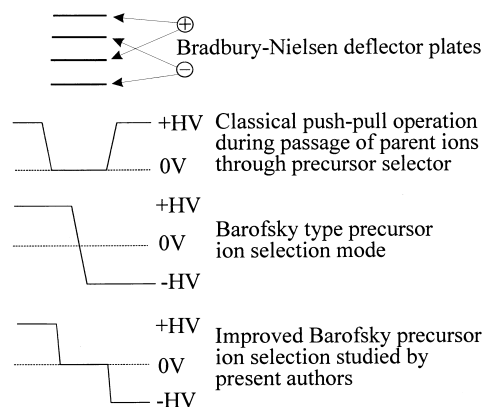


Fig. 2. Three principles of operation of a Bradbury-Nielsen type precursor ion selector. Shown is the potential switching during the passage of the parent ions through the selector. Alternative voltages are applied to consecutive plates of the deflector device.

during selected ion passage to compensate for a partial deflection, which previously occurred in the fringing field of the deflection device, or even within the deflection device. This compensation allows a shorter selection time and therefore a dramatically increased selector resolution. Because high speed switching of high voltage polarities with a halt at zero is quite a task, Barofsky and co-workers used two deflectors in series. The first deflector is used to open the gate, switching a deflection voltage to zero, and the second is used to close the gate by switching a second voltage from zero to the opposite polarity. With proper timing, the partial deflection within the first deflector is completely compensated in the second deflector. Barofsky and co-workers used an interleaved set of parallel deflection electrodes as deflectors, wired in the same way as Bradbury-Nielsen [9] gates but using small condenser plates instead of wires.

Using a single deflector of this type, Barofsky and co-workers used a voltage switched from one polarity directly to the other, with no halt at zero voltage. The mass resolution achieved here was about $m/\Delta m=700$ for ions with masses around 1300 u.

A further improvement for the single deflector results from a more sophisticated voltage generator, able to halt for a given time at zero voltage (“improved Barofsky precursor mode”). With the devel-

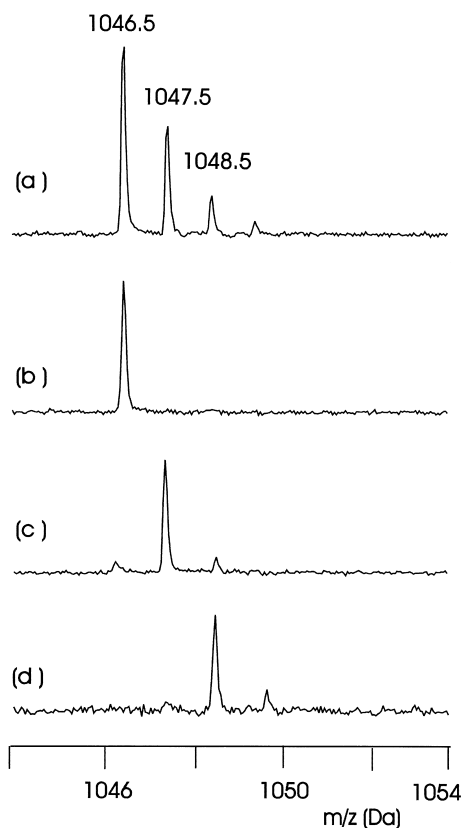


Fig. 3. Resolution achieved by the improved Barofsky-type precursor mode ion selector (with a halt at zero voltage) at threshold laser radiation, showing the isotope peaks of angiotensin II ($m/z = 1046.54$), and selections of three isotopic peaks.

opment of such an electronic device the present authors were in the position to switch off the deflection just at the moment in which the parent ions enter the deflection field. The deflection into the adverse direction is switched on when the parent ions leave the deflector. Only the deflection by the fringing fields has to be compensated. Ions entering shortly before, or after, the selected parent ions experience noncompensated deflections. Monoisotopic selection of parent ions is possible with this device using threshold laser powers (Fig. 3). For daughter ions, however, the resolution is lower due to the well-known transition of internal energy into kinetic energy during fragment ion formation. For ions in the mass range from 1000 to 6000 u, the authors achieved parent ion resolutions

from about 1000 to about 5000 full width at half height (FWHM) thus almost achieving single mass resolution sufficient to have monoisotopic precursor ion selection. A dual deflector type precursor ion selector is also described for the MALDI TOF/TOF tandem mass spectrometer described in Sec. 3.

3. Improvements of segmented PSD

As described in Sec. 2, the method of segmented PSD measurements involves the acquisition of a series of 5–20 segment spectra, each recorded at a successively reduced reflector voltage. The segment spectra are automatically pasted together by software programs to form a full daughter ion spectrum. Here we discuss the recent approaches to improve the quality, speed and sensitivity of PSD acquisition and the ease of data analysis.

3.1. Reflector design

A recent study [10] investigated the merits of diverse types of reflectors which are used in segmented MALDI PSD measurements, mainly by mathematical simulations: classical two-stage Mamyrin reflector with two grids and homogenous fields, one stage linearly decelerating reflector with only one grid, and two-stage space-focusing gridless reflector. Later the author also studied the curved field reflector (see Fig. 4).

Different reflector geometries were developed in the past to optimize their performance. For example, the grid passage of ions leads to transmission losses by collisions and, therefore, some designs avoid grids. The curved field reflector was developed to obtain the PSD spectrum in a single segment.

In the case of the single-stage gridded reflector with homogenous deceleration field, the reflector has to be very long to achieve focusing, ideally one quarter of the total field-free flight path length. Ions which pass the field-free flight path in a time period Δt , will spend about double the same time period ($2 \times \Delta t$) within the reflector field, decaying to about as many fragment ions within the reflector as in the

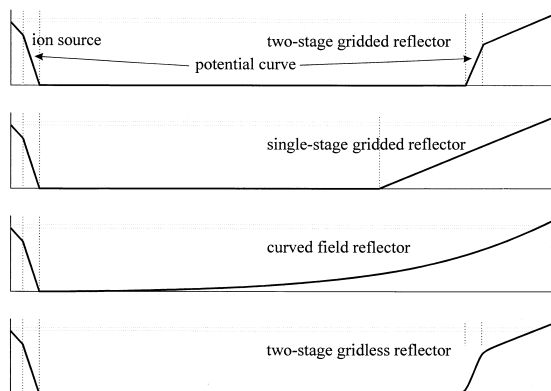


Fig. 4. Potential distributions in the various reflectors for PSD. Vertical lines indicate grids or ion optical lenses (gridless design) and horizontal lines indicate the acceleration potential and the range of similar potential gradients in the various reflectors.

field-free flight path. These fragment ions are generated within the reflector at various locations and result in a high background in the spectrum. The improvement of sensitivity by passing only one grid twice in contrast to the four grid passages in the double-stage gridded reflector is outperformed by the bad signal-to-noise ratio resulting from the high background.

Moreover, ion beams reflected by a single stage (as well as double stage) gridded reflector under a non-zero reflection angle are subject to a particularly large spatial broadening. This spatial broadening results inevitably from the fragment ion separation process in the reflector.

An ion detector with a large detection area is therefore needed for off-axis reflectors with gridded design, requiring very accurate adjustment orthogonal to the impact direction. The size requirements can only be fulfilled by a “multichannel plate” secondary electron multiplier. Further, during the acquisition of each segment spectrum, large numbers of light ions

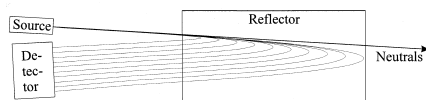


Fig. 5. In a one-stage gridded ion reflector, the fragment mass separation leads to a wide spatial broadening for nonzero angles of incidence. Due to this broadening, either larger detectors or larger numbers of segments have to be used.

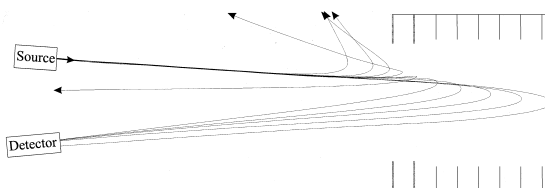


Fig. 6. In a gridless double-stage space-focusing reflector, the heavier ions (40% of the mass range under investigation) are focused onto an advantageously small detector area, whereas the lighter ions are deflected, protecting the detector from desensitization and not contributing to background signal. Thus, low noise spectra are created. The trajectories shown are calculated using SIMION.

arrive at the detector before the ions of interest, partially blinding the detection channels of the detector (see Fig. 5).

In contrast, the two-stage gridless reflector reflects 40% of the mass range under investigation into a rather small detection area, allowing for a small detector (Fig. 6). The lighter ions, not at all of interest in the acquisition of a given spectral segment, are deflected and do not arrive at the detector. Further, most of the stray ions formed by metastable decay within the reflector field do not hit the small detector area. Last but not least, multiple grid passages of the ions are avoided by the gridless reflector. Extremely high sensitivities and high signal-to-noise ratios are achieved by this design.

In this discussion, the curved field reflector must be also considered because it is the only design, which allows the acquisition of PSD spectra in a single voltage segment (see Fig. 7). It uses an approximately quadratic increase of the field strength from entrance to the end of the reflector. Whereas the two-stage reflector has the strongest field at the entrance resulting in a minimized time the ions spend inside the reflector, the curved field reflector has the weakest

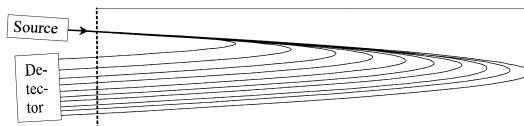


Fig. 7. SIMION trajectories of different energies in a curved field reflector. The reflector fills almost the whole flight tube. For inclined ion entry, the detector must have a large area.

fields at the entrance, maximizing the time ions spend inside the reflector. A reflector with an exact quadratic field fills the whole flight tube, i.e. the ions spend the full flight time inside the reflector. This is not very advantageous for PSD, as the ions need time on a field-free path to dissociate before they enter the reflector. Ions that fragment inside the reflector release stray ions forming a high chemical background covering a broad part of the spectrum. This reduces the sensitivity considerably although the idea of single segment PSD spectra is tempting and a driving force for other developments thus as the ones described below. However, the curved field reflector has its merits in combination with CID.

3.2. Automated calibration and data acquisition

A fuzzy logic feedback control system has been adapted to automatic PSD measurements [11]. Such a fuzzy logic feedback control system, introduced by Jensen et al. [12] and by Suckau et al. [13] into MALDI TOF mass spectrometry, has already pioneered automated MALDI measurements. It has been successfully used to control automatic acquisition of MALDI spectra for peptide mapping [14], of DNA samples [15] and of samples on large target arrays [16]. A fuzzy logic system evaluates input parameters such as mass resolution and signal-to-noise level by a set of fuzzy rules (using “fuzzy” probability values instead of simple yes/no decisions) and then generates one or more output parameters, such as laser energy and sample position, for optimum spectrum quality. After acquisition, spectra may be automatically processed including procedures such as calibration, peak annotation and database search.

Fuzzy logic applied to PSD measurements typically involves the automatic measurement of a series of up to 14 segment spectra, recorded at successively reduced reflector voltages. The automatic PSD method involves the acquisition and storage of one segment spectrum after the other under fuzzy logic optimization.

Laser energy as set by the laser attenuator and change of sample position are controlled by fuzzy logic with the height of the main peak of the segment

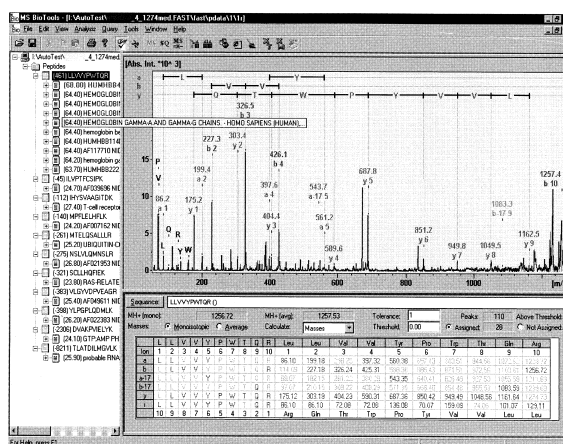


Fig. 8. Automatically recorded PSD spectrum of a tryptic in-gel digest of hemoglobin.

spectrum and the signal-to-noise level as the main evaluation parameter. Upper and lower limits of the laser pulse energies are chosen by the user. Unlike the automatic acquisition of normal mass spectra, the fuzzy logic controlled PSD spectra acquisition does not use the mass resolution as an evaluation parameter, due to the inherently different quality of the segment spectra.

After acquisition, the segment spectra are automatically calibrated and pasted to form a complete fragment spectrum, followed by peak annotation. Complete PSD measurements take about 5–15 min enabling the overnight acquisition of several dozens of PSD spectra (see Fig. 8).

The use of gridless two stage reflectors for PSD analysis used to be somewhat complicated because of its calibration. Although single stage reflectors possess a linear time of mass dependence and can be calibrated by only a few data points, two-stage gridless reflectors have to be described by a rather intricate function that is very poorly suited for conventional fits. The analysis of this function is complicated by two factors: first, the variation of peak resolution within one segment makes the automatic analysis of calibration spectra very difficult. Second, the calibration curve itself varies slightly from segment to segment, due to changes in the acquisition parameters. However, a fully automatic calibration

method was recently established that provides a reliable calibration [17].

4. PSD and CID

Metastable decomposition or PSD is a “soft” fragmentation method. During the acceleration of MALDI generated protein ions, large numbers of small energy portions are taken up by the backbone of the protein chain caused by multiple collisions with the neutral molecules in the MALDI cloud. The backbone forms a chain of coupled oscillators of different frequencies, and the energy is erratically exchanged among these coupled oscillators and transported to and fro like along a chain of coupled pendulae of different lengths. In any given moment, the energy is erratically distributed among the different oscillators. If in a given moment the energy in one of the oscillators (and the resulting drawing force) exceeds the binding energy (and force) of one oscillator bond, the bond breaks and forms an a, b, c, x, y, or z fragment, in most MALDI cases a, b, or y fragments [18]. Side chains are greatly unaffected by this process.

The degree of fragmentation can be somewhat controlled by use of different matrices and laser fluences, but there are analytes which do not fragment at all by MALDI (e.g. polymers). In addition, the SVCF with its time delay for ion acceleration produces fewer collisions of the ions with residual matrix molecules in the sample plume resulting in less PSD fragmentation. The solution to the problem is an additional collision cell providing collision gas molecules at sufficiently high pressure within the first field-free path of the ions, resulting in CID of the ions.

The high energy CID process is a “hard” fragmentation process. An ion with a kinetic energy of several kiloelectron volts collides with a stationary collision gas molecule, mostly nitrogen. The full energy is transferred to a single location of the ion. This location may be, e.g., a side chain of the peptide. In this case, the side chain is destabilized, undergoes some fast re-arrangements, and finally (after some 10 s^{-8}) a “spontaneous” fragmentation occurs, producing so-called d- or w-fragment ions, characterized

by the lack of the side chain in the terminal amino acid, amongst others. This process can be quite dominant; in some spectra, the w-fragment ions predominate the b and y ions. The production of w-fragment ions has to be built into the search algorithms for protein identification in protein sequence databases. In addition the production of small fragments is enhanced, e.g. immonium ions appear in the spectrum at significantly higher intensity. Although PSD follows the Rice-Ramsperger-Kassel-Marcus theory, CID involves nonergodic behavior [19,20].

In gridless time-of-flight mass spectrometers, the PSD and CID spectra can be differentiated by electrical means only: just by changing the focus length of the ion source lens, either the PSD ions diverting from the ion source or the CID ions diverting from the collision cell can be focused preferably onto the detector [21].

5. Unsegmented MALDI MS/MS

The disadvantages of time and sample consumption of classical segmented MALDI PSD has started several development efforts for instruments capable to acquire full PSD fragment spectra in single acquisitions: (1) the TOF/MS-MS instrument, (2) the non-linear (curved) reflector field approach mainly for CID ions, and (3) the potential lift for PSD or CID ions on the fly in a lift cell.

5.1. MALDI TOF/TOF instrument

A new design of the MALDI TOF mass spectrometer [22,23] consists of two TOF processes in tandem. It consists of a first flight path at three kilovolts, a precursor ion selector, a CID cell, a second flight path with 15 kV, and a reflector. The CID cell is at ground potential and both acceleration voltages are pulsed voltages to make use of SVCF. The selector within the first flight path yields a mass resolution of 1000; fragment resolution generally displays 2000–3000. If a method with three spectral segments is used, a fragment ion resolution up to 4000–5000 can be achieved. The instrument is suit-

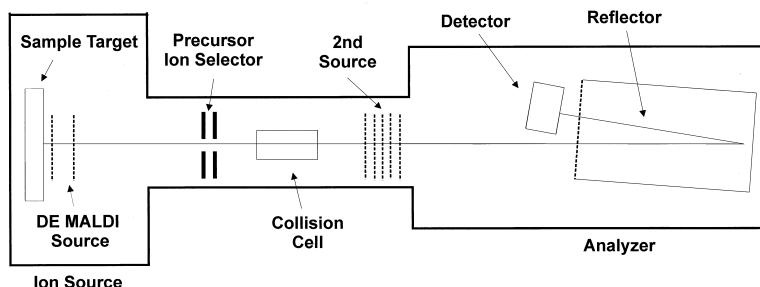


Fig. 9. Schematic diagram of the MALDI TOF-TOF instrument (not in scale).

able for digest analysis on the 100 fmol level and proteolytic peptides tandem mass spectra exhibit high numbers of w fragments typical for CID (see Fig. 9).

The first TOF reaches from the sample target to the center of the precursor ion selector. It is about 26 cm long. A 7.2 cm long collision cell at ground potential is located about 8 cm behind the ion selector. The second pulsed TOF starts at the linear acceleration stage (second source), then about 1 m of field-free drift length is followed by a 40 cm long single stage gridded reflector. As the first source operates at 3 kV, and the second source is pulsed to 15 kV, the resulting total ion energy is some hundred electron volts less than 18 keV, depending on where the ion cloud is located inside the second source, at the time the voltage is switched on. An Einzel lens is used right after the DE MALDI source to collimate the 3 keV ions in the first TOF. In the field-free drift region of the second TOF an ion guide wire is used, allowing one to choose between either optimum sensitivity or optimum resolution. The latter can be up to several thousand (FWHM) for the fragment ions. A similar instrument was shown by Barofsky and co-worker [24].

5.2. Curved field reflector

In a curved field reflector TOF, the ions are decelerated in an almost quadratically increasing reflector field. The length of such a reflector is ideally about the length of the whole TOF instrument (see Figs. 4 and 7 for details). This arrangement allows to measure all PSD fragments with the reflector detector

in a single spectrum acquisition process [25,26]. Small fragments having little energy penetrate only a short way into the reflector, large fragments penetrate a long way. Fragments with different energy all see the same shape of the reflector field (as it is quadratic) and are thus all time focused onto the detector with the same performance. Although this method easily allows to refocus all fragments simultaneously onto the detectors, it has disadvantages for PSD, as discussed in Sec. 3.1.

To minimize the necessary detector area, in such a reflector design, often detectors with a hole in the center are used through which the ions pass on their way to the reflector. The diverging reflected ion beam hits then the detector (not shown here).

The curved field reflector can advantageously be used in combination with a CID cell because the instant formation of ions by CID disables the formation of PSD ions in the reflector, therefore minimizing background noise by PSD stray ions.

5.3. Postacceleration by a potential lift device

With usual PSD, the reflector directs the ions of the upper 40% of the mass range, up to the precursor mass onto the detector. Only the ions with sufficient kinetic energy are reflected properly because only these ions penetrate into the second deceleration stage of a double stage reflector. If all the fragment ions would have at least 60% of the maximum energy, all ions would be reflected and detected in a single daughter ion spectrum.

This idea can be implemented by a postaccelera-

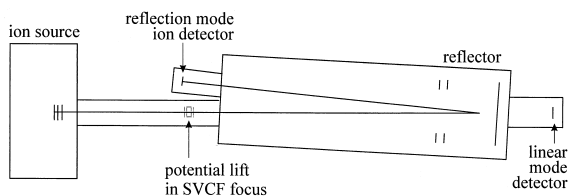


Fig. 10. Principle of reflectron TOF instrument with potential lift.

tion step affecting both, the parent and the fragment ions: In the ion source, the parent ions are only accelerated to, say, 8 keV, a much lower energy as normal. Within the field-free ion path, the parent ions partially decompose and enter a small cell, the potential of which is then suddenly lifted to a high voltage of, e.g. 12 kV. Upon exiting of the small cell, the parent and fragment ions are then accelerated by these additional 12 keV. The parent ions are thus accelerated to a total energy of 20 keV, the lightest ions to a total energy of a little over 12 keV, which is 60% of the parent energy. All ions are then properly reflected onto the detector. The full daughter ion spectrum is recorded in a single segment.

This device even selects the precursor ions because only ions which experience the potential lifting have sufficient energy to get properly reflected. The mass resolution for pre-selection, however, is relatively moderate. Therefore, it is advantageous to combine this potential lift with an improved Barofsky-type precursor ion selector.

Measurements have been performed using a prototype TOF mass spectrometry with a potential lift device in the middle of the first drift region, as outlined in Fig. 10. The cell arrangement between two grids, both at ground potential, is shown in Fig. 11. A complete PSD fragment spectrum is acquired by lifting the potential of the lift cell at the moment the precursor ion and its metastable fragment ions have entered. By the subsequent acceleration, the energies of these ions are increased by the lift cell potential and thus shifted into the operating window of the reflector.

Lift PSD fragment spectra have been obtained for various peptides. Fig. 12 shows a spectrum of ACTH, Clip 18-36 (2465.2 Da). To generate a higher yield of metastable fragments for lift spectra the laser pulse

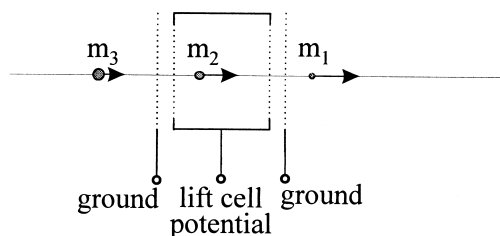


Fig. 11. Scheme of lift cell. The lift cell potential is switched to high voltage when the selected m_2 ions have entered the cell.

power has to be moderately increased. Successful database searches and peptide sequencing have been performed for lift spectra measured for peptides from trypsin digests of proteins. Even for samples in low concentration, the signal to noise is high enough. Lift spectra of digest peptides have been recorded down to the 10 fmol level.

Calibration of the lift spectra is difficult to attain, it strongly depends on the molecular mass of the parent ions. Up to now, the dependence of the calibration constants on the molecular mass has simply been considered by calibrations for three known peptides and interpolation for parent molecular masses in between, but routine calibration procedures remain to be developed. CID was not applied in the above measurements, but has proved to be useful to enhance the intensity of fragments in the low fragment mass range.

6. Chemical derivations for “de novo” sequencing

Although protein identification is very straight forward using PSD spectra of proteolytic peptides, they are usually too complicated for de novo sequencing work, which is required in all cases where, e.g. no reference sequence is in the database or in cases of modified peptides. Peptide modification reactions were regarded very useful to modify, and simplify, the fragmentation pathways for simplified data interpretation, however, quite unsuccessful until recently. By a simple single-step reaction, sulfonic acid derivatives were recently introduced by Keough et al. as an

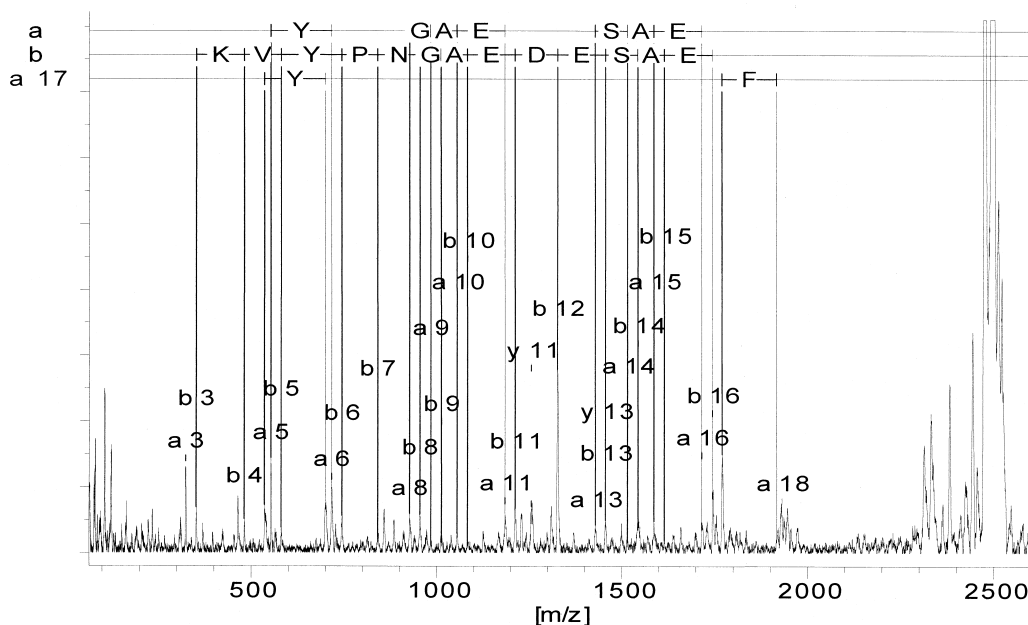


Fig. 12. Potential lift spectrum of ACTH clip 18-38.

N-terminal peptide modification, which can protonate the backbone amides in an intramolecular acid–base reaction [27]. These derivatives of tryptic peptides enhance both the fragmentation of the peptide bond and the specific detection of the γ -series ions, since the a- and b-ion formation is strongly suppressed in positive ion mode by the negatively charged N-terminal modification. As a result, the typically complex PSD spectra become more intense and much simpler to read and can be used for visual de novo sequencing. Spectra down to the 500 amol level were obtained by the authors, which were suitable for protein identification (see Fig. 13).

Modifications of peptides and digests were performed using 2-sulfobenzoic acid cyclic anhydride reacted in 50 mM NH_4HCO_3 /acetonitrile (1:1) for 1–2 min at room temperature prior to sample preparation.

All spectra were recorded using α -HCCA matrix on a reflector type MALDI-TOF mass spectrometer with precursor ion selector for PSD measurements. Spectra were evaluated with the BioTools package, including de novo sequencing evaluation. Identifications were done using the MASCOT search engine

(Matrix Science, UK) and the OWL protein sequence database on a local server with an appropriately customized N-terminal modification list.

Schnoelzer et al. [28] have published a method to ease de novo sequencing by using ^{18}O labeling. When proteins are enzymatically digested in aqueous buffers containing ^{18}O enriched water, the carboxyl functions of the resulting peptide fragments are labeled by ^{18}O . In practice, the protein sample is split and two digests are performed, one in H_2^{16}O buffer and the other one in highly enriched H_2^{18}O buffer. After incubation, the two digests are combined to yield 1:1 ion doublets of unlabeled and labeled peptide fragments. Alternately, a single digest is performed in buffers containing water with an enrichment of 50 at. % ^{18}O . This ^{18}O labeling has an important application in peptide sequencing by MALDI PSD as well as by ESI tandem mass spectrometry: fragmentation of a peptide with a labeled C-terminal carboxyl group results in labeled C-terminal fragment ions, typically those of the Y-series, whereas B-series ions representing N-terminal fragments are not labeled. Thus, when a precursor ion that exhibits a 1:1 ion doublet is fragmented, the C-

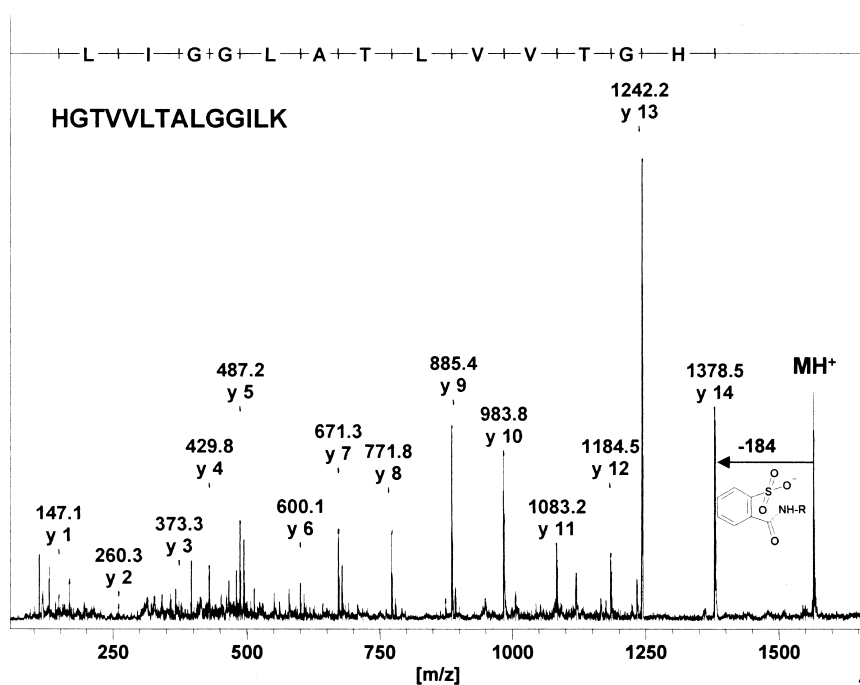


Fig. 13. Spectrum of tryptic peptide m/z 1378.8 from horse myoglobin with the typical features of PSD spectra of the modified tryptic peptides. It shows the loss $MH^+ - 184$ of the modifying group and a full y-ion series.

terminal ions show the same doublet signal as the precursor ion whereas the N-terminal fragment ions exhibit the normal isotopic pattern.

7. Vision of high throughput proteomics

Today, high throughput proteomics based on mass spectrometry is still a dream. There are lots of discussions on whether high throughput proteomics really is needed and, as usual, there are supporters and doubters.

Nevertheless, high throughput proteomics is within reach. There are automatic spot punchers for two-dimensional gels and digest robots. MALDI sample carriers were recently being developed with small hydrophilic anchors on hydrophobic surfaces. They allow for such a homogeneous and confined MALDI sample preparation that extremely high sensitivity and reproducibility is achieved across the sample area and from spot to spot [29,30]. Automatic MALDI spectra

acquisition is significantly accelerated at increased sensitivity, which increases the success rate of protein sequence library searches. The success rate of protein identification can be further increased by subsequent PSD using the same samples on the carrier. The general limitation of the PSD technique, that is precursor ions must be smaller than 4000 Da in practical life, is no problem for proteomics. However, the major limitations today are (1) rather low speed of PSD acquisitions and (2) lack of fully automated data-dependent definition of autoPSD experiments. But several industrial companies are working on this problem and techniques and software can be expected to be available soon.

But high throughput proteomics does not stop with simple protein identification. The focus of interest is already shifting toward the analysis of slight differences between different proteoms: differences between the protein isolated from a proteom and the corresponding protein in the database. Analysis of

mutations and analysis of post-translational modifications are the key issues. This task is much harder than simple protein identification: 100% sequence coverage is the goal, the low to medium coverage of present-day protein analytics has to improve further. Automatic measurements and automatic evaluation procedures have to be designed and developed to find and identify minute differences by mutations or modifications. The task list is long: let's start!

References

- [1] A.L. Burlingame, R.K. Boyd, S. J. Gaskell, *Anal. Chem.* 70 (1998) 647R.
- [2] R.J. Cotter, *Anal. Chem. News Features* July 1 (1999) 445A.
- [3] D. Kirsch, B. Spengler, R. Kaufmann, Proceedings of the 41st ASMS Conference on Mass Spectrometry, San Francisco, CA, 30 May–4 June 1993.
- [4] R. Kaufmann, D. Kirsch, B. Spengler, *Int. J. Mass Spectrom. Ion Processes* 131 (1994) 355.
- [5] S.M. Colby, T.B. King, J.P. Reilly, *Rapid Commun. Mass Spectrom.* 8 (1994) 865.
- [6] W.C. Wiley, I.H. McLaren, *Rev. Sci. Instrum.* 26 (1955) 1150.
- [7] G.R. Kinsel, J.M. Grundwürmer, J. Grottemeyer, *J. Am. Soc. Mass Spectrom.* 4 (1993) 2.
- [8] C.K.G. Piyadasa, P. Håkansson, T.R. Ariyaratne, D.F. Barofsky, *Rapid Commun. Mass Spectrom.* 12 (1998) 1655.
- [9] N.E. Bradbury, R.A. Nielsen, *Phys. Rev.* 49 (1936) 388.
- [10] A. La Rotta Angenendt, Diplomarbeit in Physik, Rheinische Friedrichs-Wilhelm-Universität, Bonn, 1999.
- [11] R. Frey, A. Holle, A. Resemann, K.O. Kräuter, R. Paape, D. Suckau, Proceedings of the 47th ASMS Conference on Mass Spectrometry and Allied Topics, Dallas, TX, 13–17 June 1999.
- [12] O.N. Jensen, P. Mortensen, O. Vorm, M. Mann, *Anal. Chem.* 69 (1997) 1706.
- [13] D. Suckau, K.-O. Kräuter, U. Rapp, M. Mann, O. Jensen, Proceedings of the 45th ASMS Conference on Mass Spectrometry and Allied Topics, Palm Springs, CA, 1–5 June 1997, p. 1057.
- [14] D. Suckau, L. Cornett, K.O. Kräuter, *Analisis* 26 (1998) M36.
- [15] M. Schürenberg, K.-O. Kräuter, D. Suckau, A. Holle, J. Höhdorf, T. Becker, D. Little, M. Shahgholi, K. Tang, 11th Sanibel Conference on Mass Spectrometry, 23–26 January 1999.
- [16] J. Höhdorf, C. Köster, A. Holle, Proceedings of the 46th ASMS Conference on Mass Spectrometry and Allied Topics, Orlando, FL, 31 May–4 June 1998, p. 1021.
- [17] A. La Rotta, A. Holle, C. Koester, K.P. Wanczek, Proceedings of the 47th ASMS Conference on Mass Spectrometry and Allied Topics, Dallas, TX, 13–17 June 1999.
- [18] K. Biemann, *Biomed. Environ. Mass Spectrom.* 16 (1988) 99.
- [19] E.W. Schlag, R.D. Levine, *Chem. Phys. Lett.* 163 (1989) 523.
- [20] L.L. Griffin, D.J. McAdoo, *J. Am. Soc. Mass Spectrom.* 4 (1993) 11.
- [21] B. Köster, US Patent No. 5,734,161 March 31, 1998.
- [22] M.A. Baldwin, K.M. Medzihradzsky, J. Campbell, X. Chen, P. Juhasz, M.L. Vestal A.L. Burlingame, Proceedings of the 47th ASMS Conference on Mass Spectrometry and Allied Topics, Dallas, TX, 13–17 June 1999.
- [23] K.F. Medzihradzsky, J.M. Campbell, M.A. Baldwin, A.M. Falick, P. Juhasz, M.L. Vestal, A.L. Burlingame, *Anal. Chem.* 72 (2000) 552.
- [24] C.L. Katz, D.F. Barofsky, Proceedings of the 47th ASMS Conference on Mass Spectrometry and Allied Topics, Dallas, TX, 13–17 June 1999.
- [25] T.J. Cornish, R.J. Cotter, *Rapid Commun. Mass Spectrom.* 8 (1994) 781.
- [26] A.S. Woods, D.P. Little, T. Cornish, R.J. Cotter, *J. Mass Spectrom. Soc. Jpn.* 46 (1998) 91.
- [27] T. Keough et al., *Proc. Natl. Acad. Sci. USA* 96 (1999) 7131.
- [28] M. Schnoelzer, P. Jedrzejewski, W.D. Lehmann, *Electrophoresis* 17 (1996) 945.
- [29] M. Schürenberg, C. Luebbert, H. Eickhoff, M. Kalkum, H. Lehrach, E. Nordhoff, *Anal. Chem.*, 72 (2000) 3436.
- [30] M. Schürenberg, S. Hahner, E. Nordhoff, D. Suckau, Proceedings of the 46th ASMS Conference on Mass Spectrometry and Allied Topics, Orlando, FL, 31 May–4 June 1998, p. 1005.